NewsStand, Inc. - Today's Way To Read Publications--Digitally - Microsoft Internet Explorer

9. Levine, D. & Steinhardt, P. J. Quasicrystals: a new class of ordered structures. *Phys. Rev. Lett.* **53**, 2477–2480 (1984).
10. Steinhardt, P. J. & Ostlund, S. *The Physics of Quasicrystals* (World Scientific, Singapore, 1987).
11. Pierce, F. S., Poon, S. J. & Biggs, B. D. Band-structure gap and electron transport in metallic quasicrystals and crystals. *Phys. Rev. Lett.* **70**, 3919–3922 (1993).
12. Fujiwara, T. & Tsuei tsugu, H. in *Quasicrystals: The State of the Art* (eds DiVincenzo, D. P. & Steinhardt, P. J.) 2nd edn 361–390 (World Scientific, Singapore, 1999).
13. Johnson, S. G. & Joannopoulos, J. D. Block-iterative frequency-domain methods for Maxwell's equations in a planewave basis. *Opt. Express* **8**, 173–190 (2001).
14. Zeng, X. C., Bergman, D. J., Hui, P. M. & Stroud, D. Effective-medium theory for weakly nonlinear composites. *Phys. Rev. B* **38**, 10970–10973 (1988).

Acknowledgements We thank N. Jarosik for his extensive help on microwave measurements. We thank I. Aksay and the Chemical Engineering Department for the use of their SLA system, and the Gravity Group of the Princeton Physics Department for use of their microwave transmission measurement equipment. We also thank O. Crisafulli and R. Yang for help in the numerical aspects. This research was supported by NASA, by the US Department of Energy and by the National Science Foundation.

Author Information Reprints and permissions information is available at npg.nature.com/reprintsandpermissions. The authors declare competing financial interests: details accompany the paper on www.nature.com/nature.
Correspondence and requests for materials should be addressed to P.J.S. (steinh@princeton.edu).

Vol 436|18 August 2005|doi:10.1038/nature03932 nature

LETTERS

Liquid crystal 'blue phases' with a wide temperature range

Harry J. Coles[1] & Mikhail N. Pivnenko[1]

Liquid crystal 'blue phases' are highly fluid self-assembled three-dimensional cubic defect structures that exist over narrow temperature ranges in highly chiral liquid crystals[1]. The characteristic period of these defects is of the order of the wavelength of visible light, and they give rise to vivid specular reflections[2] that are controllable with external fields[3,4]. Blue phases may be considered as examples of tuneable photonic crystals[5] with many potential applications. The disadvantage of these materials, as predicted theoretically and proved experimentally[1], is that they have limited thermal stability: they exist over a small temperature range (0.5–2 °C) between isotropic and chiral nematic (N*) thermotropic phases, which limits their practical applicability. Here we report a generic family of liquid crystals that demonstrate an unusually broad body-centred cubic phase (BP I*) from 60 °C down to 16 °C. We prove this with optical texture analysis, selective reflection spectroscopy, Kössel diagrams and differential scanning calorimetry, and show, using a simple polarizer-free electro-optic cell, that the reflected colour is switched reversibly in applied electric fields over a wide colour range in typically 10 ms. We propose that the unusual behaviour of these blue phase materials is due to their dimeric molecular structure and their very high flexoelectric coefficients. This in turn sets out new theoretical challenges and potentially opens up new photonic applications.

There are three well-known[1] thermodynamically stable blue phases, BP III*, BP II* and BP I*, observed on cooling from the isotropic phase to the chiral nematic phase. BP III* is amorphous with a local cubic lattice structure in the director field, whereas BP II* and BP I* have a fluid three-dimensional periodic structure in the director field with simple cubic and body-centred cubic symmetry, respectively. For BP I* and BP II* the lattice periods are of the order of the wavelength of visible light and give rise to selective 'Bragg reflections'. These lead to potentially interesting photonic applications, such as three-dimensional blue-phase lasers[10]. Further, because of the fluidity of blue phases, external fields may be used to induce changes in the lattice parameters, thereby changing the specular reflection; this has led to simple colour change devices and optical filters. Hitherto, as predicted theoretically and observed experimentally, neat blue phases have only existed over a narrow temperature range a few degrees Celsius wide and this has limited such practical applicability. Several attempts have been made to widen the temperature interval of the blue phases, notably by polymer stabilization[11,12]; the most recent report describes the stabilization of the three-dimensional cubic lattice in a defect confined polymer matrix[13]. Although an electro-optic Kerr effect, that is, a field-induced birefringence, was observed in an external electric field, this arose from the regions between the defect or disclination lines[14], and the polymer lattice clearly restricted the deformation of the blue-phase lattice. Hence, no colour switching was observed.

In this paper, we describe novel blue-phase materials (BP I* and BP II*) that are stable over a 40–50 °C temperature range, in which their reflectance band is switched linearly in an external field through deformation of the defect lattice, to give any desired reflectance colour at ambient temperatures. An electro-optic response with switching times of 10–40 ms and relaxation times of ~1–10 ms, depending on temperature, is also detected. We have so far made some 30 different mixtures that show blue phases 40–50 °C wide using both symmetric and non-symmetric bimesogens. The generic structure of our bimesogens is shown in Fig. 1a and for a typical blue-phase mixture of the type we describe here we use mixtures of the ratio 30.4% ($n = 7$), 35.1% ($n = 9$), 30.6% ($n = 11$) with 3.9% of the high twisted power (HTP) agent BDH1281 (available from Merck Chemicals and described in ref. 15). All concentrations are w/w and n refers to the number of methylene spacers in the alkyl chain linking the two mesogenic structures. The mixtures were studied by polarizing optical microscopy, light diffraction (Kössel diagrams), differential scanning calorimetry and electro-optic spectroscopy. The materials were contained in parallel plate glass cells with 7.0, 15 and 50-μm cell gaps and 4 mm × 4 mm indium-tin-oxide pixel electrodes. There were no alignment layers on the electrodes. The mixture showed the following phase sequence: isotropic 57.72 °C BP III*, 57.58 °C BP II*, 57.22 °C BP I*, 16.5 °C SmX* and −28 °C glass phase, where SmX* is an, as yet, unidentified smectic phase. The cooling rate was 0.001 °C min^{-1} from the isotropic phase down to 56.84 °C to allow us to identify the phase transitions accurately, and then at 0.5 °C min^{-1}. Figure 1b, c, d shows the classical BP I* texture observed in our mixture on forming at 57.24 °C and then on cooling through 41 °C to 25 °C, some 32 °C below the BP II*–BP I* transition. To ensure that this was not a supercooled BP I*, we maintained the cell at 22–25 °C for over four months, and this texture remained unchanged irrespective of the sample thickness. Clearly the BP I* is identical at 41 °C and 25 °C and apart from some slight reflection-colour changes between 57.24 °C and 56.7 °C (see Fig. 2a), the platelet texture is identical. Further, on placing the sample between crossed polarizers and rotating the sample in plane the textures remain identical. This confirms that the reflected colours come from specular lattice reflections and not birefringence phenomena. We then indexed these lattice parameters using the Kössel diagram technique[16]. In Fig. 1e we give the Kössel diagrams and indexing for two specific platelets at 25 °C. These are identical to those recorded at higher temperatures up to the transition region of 56.7 °C. Differential scanning calorimetry measurements, on thermal cycling, confirmed the stability of these phases and the data are given in the Supplementary Fig. 1 along with textures for the BP I*, BP II* and BP III* phase transitions (Supplementary Fig. 2). Textures for the BP I* phase in a 50-μm-thick sample are given in Supplementary Fig. 3, confirming that the stability of the BP I* is not due to super cooling or due to sample thickness.

Given that the optical textures are classical blue phases over such a wide temperature range and that the lattice periodicities could be

[1]Centre of Molecular Materials for Photonics and Electronics, Engineering Department, University of Cambridge, Trumpington Street, Cambridge CB2 1PZ, UK.

NATURE 08/18/2005 Section: Letters to Nature Page: 996/997
Интернет
пуск NewsStand, I... NewsStand, I... Microsoft Word Adobe Acrob... EN 9:44

NewsStand, Inc. - Today's Way To Read Publications--Digitally - Microsoft Internet Explorer

indexed using Kössel diagrams, we examined the spectral, thermo- and electro-optic properties in more detail. We repeated the same cycle of cooling from the isotropic phase through the BP II* and BP I* phases (Fig. 2a, b). BP II* gives a near-ultraviolet reflection which decreases in wavelength on cooling, commensurate with a lattice contraction. At the BP II*–BP I* transition the lattice parameter increases to give a 60-nm increase in the reflection band, which then gradually increases over a 0.4 °C temperature range and then maximizes at ~500 nm (that is, green reflected light; Fig. 2a). On further cooling, over a ~40 °C range, this (200) reflection wavelength then very gradually decreased, by only 10 nm, until the SmX* phase is reached (Fig. 2b). We also monitored the (110) reflection from a 'red' platelet which showed exactly the same behaviour (Fig. 2b). The insets for Fig. 2a, b show the classical narrow linewidth associated with reflections from blue phases. By adjusting the concentration of chiral additive we altered the pitch of the system to give red, green and blue reflections in BP I; these are compared with a typical chiral nematic using the same chiral additive in Fig. 2c. All sets of data are at 25 °C and it is clear that the narrow spectral lines of the blue phases give much narrower linewidths and higher reflection intensities than the chiral nematic at the same temperature. From these data sets—that is, the optical textures, the Kössel diagrams, the differential scanning calorimetry and the spectral linewidths—it is clear that we observed blue phases over a 40–50-K-wide temperature range, in pure mixtures unaided by supercooling effects achieved using polymer networks[13].

We then studied the electric-field dependency of the selective reflection in BP I* at 25 °C by applying increasing and then decreasing pulsed alternating current (a.c.) electric fields (100 Hz; Fig. 3a). This shows two very distinct regimes. For fields below 14 V μm^{-1}, with increasing field strength, there is a gradual decrease in reflected wavelength from ~572.5 nm down to 568 nm with a small residual hysteresis (<1 nm) between increasing and decreasing field. This is consistent with small changes in refractive index due to local director orientation within the (110) lattice. However, above the critical or threshold field for these materials, the reflected colour changes rapidly from red/orange to green/blue (that is, 572 nm to 506 nm) as the field is increased to 18 V μm^{-1}. On removal of the field the green/blue reflected colour reverted back to red/orange. The hysteresis between increasing and decreasing field is very small (a few nanometres). This dramatic field-switchable colour is shown in Fig. 3b. As shown in Fig. 3a, the reflected wavelength is linearly dependent on field in this field regime (that is, between 14 V μm^{-1} and 18 V μm^{-1}). These changes are quite clearly due to electric-field-induced lattice distortions; that is, electrostriction. Further, up to the start of the transition from BP I*–BP II* these wavelength changes are independent of temperature to within a few nanometres. The reflection images recorded in Fig. 3b are for typical pixel-sized indium-tin-oxide electrodes (that is, 50 μm × 50 μm) of a dot matrix array on glass substrates. On application of a pulsed a.c. field (100 Hz) the lattice distortion has a rise time of 53 ms (at 30 °C) in response to a 14 V μm^{-1} (root mean square, r.m.s.) field and on removal of the field the decay or fall time back to the undisturbed lattice was 7 ms. As the temperature is increased for the same field these response times decrease on a logarithmic scale so that at ~40 °C the rise time is 20 ms and the fall time drops to ~3 ms (Fig. 3c).

To understand the origins of these blue-phase materials and their properties we consider the macroscopic behaviour of the bimesogens in more detail. We recently discovered[17] that these bimesogens give rise to the highest recorded (an order of magnitude greater than for monomesogens) flexoelectro-optic ratios (e/k) in the chiral nematic phase (N*). In the flexoelectro-optic effect[18] a chiral nematic is constrained to lie in the plane of a simple electro-optic device, formed by the two glass substrates with indium-tin-oxide electrodes on each face, hybrid alignment layers and the N* material positioned between the substrates. On application of an electric field, the optic axis rotates in the plane of the device by an angle φ defined by $\tan\varphi = \frac{e}{k}E$, where e is the average of the flexoelectric coefficient, k is the average of the splay and bend elastic constant, K is the helical wave vector $2\pi/p$ (where p is helix pitch) and E is the applied field. The figure of merit here is e/k. In bimesogenic mixtures similar to those described herein[19] we have now achieved switching angles of ±86°, which implies a very high e/k for these bimesogenic materials. We have also measured high k values compared to 'normal' nematic liquid crystals, so these bimesogens can readily deform in the director field to give extraordinarily high values of e. It is the demonstration of the high e and k values associated with the bimesogens, when incorporated into short-pitch chiral structures, that led us to examine the blue phases formed by these materials. The large flexoelectric effect arises from the distortion of the rapidly varying director field in the chiral nematic phase and similar distortions must be present in BP I* and BP II* at the site of the line singularity ($s = -1/2$) formed by the intersection of the three orthogonal double twist cylinders characteristic of the blue phases[1]. We believe that it is the large localized flexoelectric polarization generated by such director distortions close to these disclination line singularities that stabilizes the blue phases with the bimesogenic materials and effectively 'pins' the lattice defects. Macroscopically, owing to symmetry, the net polarization will be zero when averaged around the singularity.

Here we report naturally occurring broad-temperature-range blue-phase materials that demonstrate large analogue reflected-colour switching induced in electric fields with response times of a few milliseconds. The zero-field reflected colour is chosen by the concentration of HTP chiral additive (see Fig. 2c). The pixellated test device did not incorporate polarizers, analysers or colour filters and we believe that these materials will lead to a new generation of transreflective bright, low-power-consumption liquid crystal displays[20]. Further, the use of voltage-controlled colour means that each pixel can reflect red, green or blue (RGB) using temporal dither and reduce the pixel and thin film transistor (TFT) density by a factor of three. The materials may also be used in tuneable optical filters.

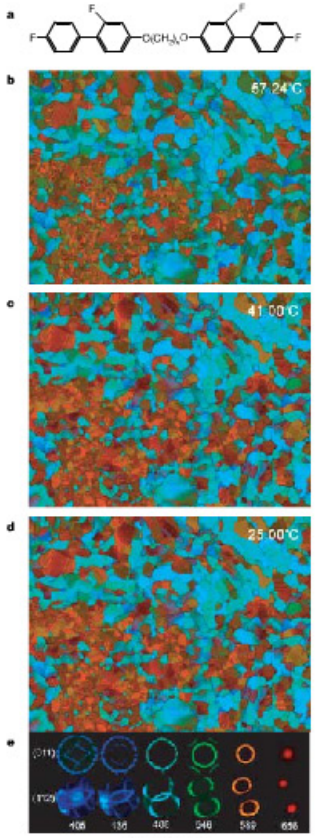

Figure 1 | Blue phase materials, temperature dependence of optical textures and Kössel diagrams. **a**, Generic chemical structure of the materials. **b–d**, Typical textures of the BP I* phase over a temperature range from 57 °C to 25 °C in a 7-μm cell with cooling rate of 0.5° min^{-1}. **e**, The Kössel diagrams for the domains in (011) and (112) orientations for different wavelengths.

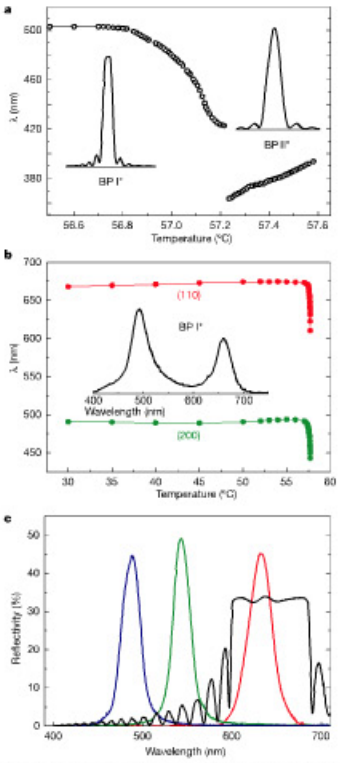

Figure 2 | Spectral properties of blue phases as a function of temperature and composition. **a**, Temperature dependence of the wavelength of the Bragg reflection for the BP I* and BP II* phases over a narrow temperature range and a typical shape of the reflection spectra (insert). **b**, Temperature dependence of the wavelength of the Bragg reflections for two domains of (110) and (200) orientation of the BP I* phase over a broad temperature range. **c**, Selective reflection spectra in the BP I* phase at 25 °C for mixtures with 3.9, 4.8 and 5.3% concentration of the chiral additive (red, green and blue spectral lines, respectively), and the selective reflection spectrum in the N* phase (black line) for a commercially available material E49 with the same chiral additive.

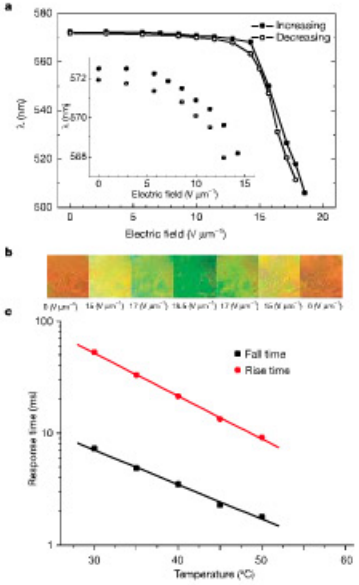

Figure 3 | Voltage- and time- dependent colour switching of BP I*. **a**, Electric-field dependence of the selective reflection peak for BP I* at 25 °C. **b**, Colour switching of an individual display pixel observed on reflection as a function of applied field in BP I at 25 °C. **c**, The temperature dependence of the rise and fall response times observed between crossed polarizers. The inset shows an expanded plot of the selective reflection as a function of the applied electric field at low fields (that is, below 14 V μm^{-1}). The axis labels are the same for both plots.

NATURE 08/18/2005 Section: Letters to Nature Page: 998/999
Интернет
пуск NewsStand, I... NewsStand, I... Microsoft Word 1808 8.pdf EN 9:44

NewsStand, Inc. - Today's Way To Read Publications--Digitally - Microsoft Internet Explorer

Further, because of the photonic bandgap nature of BP I, the materials may also readily be incorporated into three-dimensional organic lasers[10] but with a wide temperature range of stability. The electric-field-induced lattice distortions will add a new generation of continuously tuneable laser sources and indeed opens up new perspectives for liquid-crystal-based photonics.

Received 3 March; accepted 8 June 2005.

1. Crooker, P. P. in *Chirality in Liquid Crystals* (eds Kitzerow, H.-S. & Bahr, C.) 186–222 (Springer, New York, 2001).
2. Stegemeyer, H. *et al.* Thermodynamic, structural and morphological studies on liquid-crystalline blue phases. *Liq. Cryst.* **1,** 3–28 (1986).
3. Gleeson, H. F., Simon, R. & Coles, H. J. Electric field effects and two frequency colour switching in the cholesteric and blue phases of nematic/cholesteric mixtures (Tenth Int. Liquid Crystal Conf. (York, UK, July 1984; Paper G17). *Mol. Cryst. Liq. Cryst.* **129,** 37–52 (1985).
4. Gerber, P. R. Electro-optical effects of a small pitch blue phase system. *Mol. Cryst. Liq. Cryst.* **116,** 197–206 (1985).
5. Coles, H. J. & Gleeson, H. F. Electric field induced phase transitions and colour switching in the blue phases of chiral nematic liquid crystals. *Mol. Cryst. Liq. Cryst.* **167,** 213–225 (1989).
6. Dmitrienko, V. E. Electro-optic effects in blue phases. *Liq. Cryst.* **5,** 847–851 (1989).
7. Kitzerow, H.-S. The effect of electric fields on blue phases. *Mol. Cryst. Liq. Cryst.* **202,** 51–83 (1991).
8. Heppke, G., Jerome, B., Kitzerow, H.-S. & Pieranski, P. Electrostriction of the cholesteric blue phases BP I BP II in mixtures with positive dielectric anisotropy. *J. Phys.* **50,** 2291–2298 (1991).
9. Etchegoin, P. Blue phases of cholesteric liquid crystals as thermotropic photonic crystals. *Phys. Rev. E* **62,** 1435–1437 (2000).
10. Cao, W., Muñoz, A., Palffy-Muhoray, P. & Taheri, B. Lasing in a three-dimensional photonic crystal of the liquid crystal blue phase II. *Nature Mater.* **1,** 111–113 (2002).
11. Kitzerow, H.-S. *et al.* Observation of blue phases in chiral networks. *Liq. Cryst.* **14,** 911–916 (1993).
12. Bohley, C. & Scharf, T. Blue phases as photonic crystals. *Proc. SPIE* **5184,** 202–208 (2003).
13. Kikuchi, H., Yokota, M., Hisakado, Y., Yang, H. & Kajiyama, T. Polymer-stabilized liquid crystal blue phases. *Nature Mater.* **1,** 64–69 (2002).
14. Hisakado, Y., Kikuchi, H., Nagamura, T. & Kajiyama, T. Large electro-optic Kerr effect in polymer stabilised liquid-crystalline blue phases. *Adv. Mater.* **17,** 96–98 (2005).
15. Parry, O., Nolan, P., Farrand, L. & May, A. L. Chiral dopants. UK Patent GB2329636 (31 March 1999).
16. Pieranski, P. in *Chirality in Liquid Crystals* (eds Kitzerow, H.-S. & Bahr, C.) 28–66 (Springer, New York, 2001).
17. Coles, H. J., Coles, M. J., Perkins, S. P., Musgrave, B. M. & Coates, D. Bimesogenic compounds and their use in flexoelectric liquid crystal devices. UK Patent GB2356629 (30 May 2001).
18. Patel, J. S. & Meyer, R. B. Flexoelectric electro-optics of a cholesteric liquid crystal. *Phys. Rev. Lett.* **58,** 1538–1540 (1987).
19. Coles, H. J., Clarke, M. J., Morris, S. M., Broughton, B. J. & Blatch, A. E. Strong flexoelectric behaviour in bimesogenic liquid crystals. *J. Appl. Phys.* (submitted).
20. Wu, S. T. & Yang, D.-K. *Reflective Liquid Crystal Displays* Ch. 1 (Wiley, Chichester, UK, 2002).

Supplementary Information is linked to the online version of the paper at www.nature.com/nature.

Acknowledgements H.J.C. thanks the EPSRC, UK, who funded the materials research under their Displays and Functional Materials initiatives.

Author Contributions H.J.C. invented the flexoelectric materials, was responsible for the project planning, wrote the Letter and was responsible for the tentative explanation. M.N.P. carried out all the experimental work, including microscopic texture and data analysis.

Author Information Reprints and permissions information is available at npg.nature.com/reprintsandpermissions. The authors declare no competing financial interests. Correspondence and requests for materials should be addressed to H.J.C. (hjc37@cam.ac.uk).

LETTERS

Short-term variations in the oxidizing power of the atmosphere

Martin R. Manning[1], David C. Lowe[2], Rowena C. Moss[2], Gregory E. Bodeker[2] & William Allan[2]

The hydroxyl radical is the predominant atmospheric oxidant[1], responsible for removing a wide range of trace gases, including greenhouse gases, from the atmosphere. Determination of trends and variability in hydroxyl radical concentrations[2,3] is critical to understanding whether the 'cleansing' properties of the atmosphere are changing. The variability in hydroxyl radical concentrations on annual to monthly timescales, however, is difficult to quantify. Here we show records of carbon monoxide containing radiocarbon (^{14}CO), which is oxidized by hydroxyl radicals[4,5], from clean-air sites at Baring Head, New Zealand, and Scott Base, Antarctica, spanning 13 years. Using a model study, we correct for known variations in production of ^{14}CO (refs 6, 7), allowing us to exploit this species as a diagnostic for short term changes in hydroxyl radical concentrations. We find no significant long-term trend in hydroxyl radical concentrations but provide evidence for recurring short-term variations of around ten per cent persisting for a few months. We also find decreases in hydroxyl radical concentrations of up to 20 per cent, apparently triggered by the eruption of Mt Pinatubo in 1991 and by the occurrence of extensive fires in Indonesia in 1997.

^{14}CO is produced in the atmosphere by cosmic-ray-induced neutrons and has an atmospheric lifetime of about three months. Extensive measurements of ^{14}CO became practical after technical advances[8–11] in the late 1980s. Here we consider the two longest records of ^{14}CO based on these methods, which are from Southern Hemisphere clean-air sites at Baring Head (41.4° S), New Zealand, and Scott Base (77.8° S), Antarctica, and cover 1989 to 2003. Our focus is on the ^{14}CO produced directly from ^{14}C, so we remove a 'recycled' fraction[11] due to surface emissions of CO containing ^{14}C and oxidation of atmospheric $^{14}CH_4$ to ^{14}CO (see Methods). These corrections typically amount to 20% of the measured values and result in a 'primary' ^{14}CO concentration directly attributable to recent ^{14}C production.

Figure 1 shows primary ^{14}CO concentrations from our two sites and three features are evident. First, there is a large seasonal cycle of about ±40% around the annual mean owing to the strong seasonality of hydroxyl radicals (OH) at these latitudes together with the sensitivity of ^{14}CO to OH variations. For comparison, the seasonal cycle of the longer-lived methylchloroform species, also used to diagnose OH, varies by about ±3% around its annual mean. Second, annual mean ^{14}CO concentrations varied by more than 50%, reflecting solar modulation of ^{14}C production[6] during the last Schwabe cycle and apparently following independently estimated ^{14}C production rates[7] for the period. Third, despite their large latitudinal separation, concentrations at the two sites generally agree to within 1 molecule cm^{-3}, although in some years Antarctic

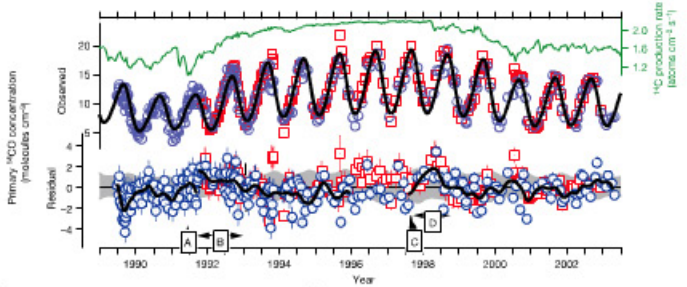

Figure 1 | ^{14}CO data and simulation. The upper section shows primary ^{14}CO concentrations for individual samples from Baring Head (blue circles) and Scott Base (red squares) from 1989 to 2003. The green and black curves show ^{14}C production rates (right-hand scale) and the best-fit simulation of ^{14}CO discussed in the text. The lower section shows residuals (observed minus simulated), measurement uncertainties (1-σ), and a Reinsch spline smooth curve, fitted separately to residuals before and after the discontinuity in September 1991, and masked out during 1996 and 1997—when the sites differ as discussed in the text. The grey shaded region shows the deviations from the best fit that would be caused by a 10% reduction or increase in OH concentrations. A, time of eruption of Mt Pinatubo; B, period of high Southern Hemisphere CH_4 concentrations[17]; C, time profile of Indonesian fires[18]; and D, period of high Southern Hemisphere CO concentrations[19].

[1]IPCC Working Group I Support Unit, Boulder, Colorado 80305, USA. [2]National Institute of Water and Atmospheric Research, Wellington 6003, New Zealand.

NATURE 08/18/2005 Section: Letters to Nature Page: 1000/1001
Интернет
пуск NewsStand, I... NewsStand, I... Microsoft Word 1808 8.pdf EN 9:45